Materials Research, Vol. 11, No. 1, 1-9, 2008

Influence of Cathodic Current Density and Mechanical Stirring on the Electrodeposition of Cu-Co Alloys in Citrate Bath

Leandro Trinta de Farias, Aderval Severino Luna,

*Dalva Cristina Baptista do Lago, Lilian Ferreira de Senna**

Departamento de Química Analítica, Instituto de Química,
Universidade do Estado do Rio de Janeiro – UERJ, Rua São Francisco Xavier, 524,
Pavilhão Haroldo Lisboa, Sala 427, Maracanã, 20550-013 Rio de Janeiro - RJ, Brazil

Received: August 22, 2006; Revised: March 17, 2008

Cathodic polarization curves of Cu-Co alloys were galvanostatically obtained on a platinum net, using electrolytes containing copper and cobalt sulfates, sodium citrate and boric acid (pH values ranging from 4.88 to 6.00), with different mechanical stirring conditions. In order to evaluate quantitatively the influence of the applied current density and the mechanical stirring on the cathodic efficiency, the alloy composition for the Cu-Co alloy deposition process, and the average deposition potential, an experimental central composite design 2^2 was employed, and three current density intervals (0.11 to 0.60, 0.50 to 1.98 and 2.44 to 9.94 $mA.cm^{-2}$) were chosen from the polarization curves for this purpose. The results indicated that the current density (mainly in the range between 0.11 and 0.60 $mA.cm^{-2}$) affected significantly all the studied variables. In the intermediate range (0.50 to 1.98 $mA.cm^{-2}$), only the average potential was influenced by the current density. On the other hand, the mechanical stirring had a significant effect only on the copper content, for both the lowest (0.11 to 0.60 $mA.cm^{-2}$) and the highest current density range (2.44 to 9.94 $mA.cm^{-2}$). Indeed, in the last range, none of the studied deposition parameters presented significant influence on the studied variables, except for the copper content. This could probably be explained by the direct incorporation of Cu-Citrate complexes in the coating, which was enhanced at high current values.

Keywords: *copper-cobalt alloy electrodeposition, citrate electrolytes, experimental design*

1. Introduction

Metallic coatings are generally applied to a substrate surface in order to produce a coating/substrate system with enhanced mechanical, magnetic, optical or anticorrosive properties. Cu-Co alloys, deposited on copper, platinum or silicon substrates, have been presenting great interest due to their possible use in data store systems and sensor technology[1-3]. The above mentioned applications are based on the giant magneto resistance properties presented by these alloys, which promotes a great variation of electrical resistance in an external magnetic field. However, these properties can only be observed in a metastable solid solution containing few amounts of cobalt in a copper matrix, enhancing the segregation of small Co precipitates, forming a granular alloy. These alloys can also find a suitable application for catalytic purposes[4-6] and anticorrosive coatings[7,8].

Several deposition processes have been studied to produce Cu-Co alloys. The physical vapor deposition (PVD) and chemical vapor deposition (CVD) methods are the most used among all of them. A simpler and less expensive alternative to obtain Cu-Co alloy coatings uses electrodeposition[9,10]. However, the alloy electrodeposition process is more complex than the single metal deposition and involves the control of a greater number of chemical and operational parameters. Industrially, these parameters are generally chosen empirically. Therefore, it is important to develop a more scientific approach leading to a better fundamental understanding of the alloy deposition phenomenon. This could be obtained using experimental design and statistical approaches[11-13], which would make it possible to improve both, the process performance and the reliability, as well as to establish new alloys systems.

*e-mail: lsenna@uerj.br

High quality metallic alloy can be obtained by using complex agents, which diminish the activity of the nobler metallic ion in solution[14-16]. Consequently, the proximity of the potentials of the metal ions can then be attained[15,16]. Cyanide has been conventionally used as the complexing agent in Cu-alloys electrolytes[4,16,17], despite the high toxicity and the need of a rigorous maintenance and control of solutions. Several alternatives to the conventional cyanide electrolytes can be found in the literature, based on glycinate[4], pyrophosphate[18], and mainly citrate[9,10,19] ions as complexing agents, producing good quality Cu-Co alloys with variable chemical compositions. Citrate is the most studied complexing agent for Cu-alloys. It is important to point out, however, that neither the chelation mechanism, nor the electroplating process have yet been wholly clarified for most of the Cu-alloys in citrate baths, these being dependent on several parameters such as the stability of the metal ion/citrate complex, the citrate concentration and the medium pH[20-22]. Chaissang et al.[20] proposed that the discharge of the copper-citrate complexes in citrate concentration range from 0.5 to 0.8 $mol.L^{-1}$ and pH close to 5.0 might occur as follows:

$$[CuCitH] + 2e^- \rightarrow [CuCitH]^{2-} \quad (1)$$

$$[CuCitH]^{2-} \rightarrow Cu + H^+ + [Cit]^{3-} \quad (2)$$

$$[CuCitH]^{2-} \rightarrow \text{included species} \quad (3)$$

$$[Cit]^{3-} \rightarrow [Cit]^{3-}_{sol} \quad (4)$$

$$[Cit]^{3-} \Leftrightarrow [Cit]^{3-}_{ads} \quad (5)$$

In this mechanism, the complexes [CuCitH] are reduced without previous dissociation (Reaction 1). The reduced copper complexes, $[CuCitH]^{2-}$, can follow two pathways: it can be dissociated on the electrode surface (Reaction 2) or be directly incorporated to the deposit (Reaction 3). The real composition of the included species is not known. As a consequence of Reactions 2 and 3, the electrode surface will present an excess of free complexing agent, $[Cit]^{3-}$ and/or some included specie, which can block a fraction of this area[20,21]. The anion $[Cit]^{3-}$ can also diffuse to the bulk, and probably complex metallic species (Reaction 4). The direct inclusion of reduced copper complexes (Reaction 3) is generally assumed to be proportional to the applied current and to the surface concentration of $[CuCitH]^{20}$.

The model proposed by Rode et al.[21] is qualitatively in agreement with the suggestion of Chaissang et al.[20] concerning the existence of an adsorbed species generated at the electrode surface during the reduction, which could block the surface and increase the overpotential. However, they suggest that the adsorbed/blocking species is $Cu_2Cit_2H^{6-}_{-2\ (ads)}$, and not the Cit^{3-} ion, as shown in Reaction 5. Therefore, their proposed model is presented as follows:

$$Cu^{2+} + 2e^- \rightarrow Cu \quad (6)$$

$$CuCit^- + 2e^- \rightarrow Cu + Cit^{3-} \quad (7)$$

$$Cu_2Cit_2H^{4-}_{-2} + 2e^- \rightarrow Cu_2Cit_2H^{6-}_{-2\ (ads)} \quad (8)$$

$$Cu_2Cit_2H^{6-}_{-2\ (ads)} + 2e^- + H_2O \rightarrow 2\ Cu + 2Cit^{3-} + 2\ OH^- \quad (9)$$

Reactions 6 and 7 are the direct discharge onto available (non-blocked) sites of free cupric ion and of the $CuCit^-$ pseudospecies, respectively. Reactions 8 and 9 present a two-step discharge for the $Cu_2Cit_2H^{6-}_{-2}$ dimer ion, passing through an adsorbed blocking intermediate. The influence of pH in copper deposition potentials was also verified, although no influence of the citrate concentration on this variable could be noted. Uksene et al.[22] also noted that the pH range studied determined the kind of Cu-citrate complex taking part in the charge transfer process. Therefore, in alkaline medium the CuL^{2-} complex predominates, while in acidic medium the $CuLH^-$ species takes part in the charge transfer step.

On the other hand, the deposition of Co-alloys in citrate bath can be an anomalous process (e.g. Co-Ni[23] alloys) or not, as can be noted for Cu-Co and Sn-Co alloys[24]. In the case of these last mentioned alloys, Co-alloys can be obtained from both complexed and uncomplexed species, as follows[8]:

$$Co^{2+} + 2e^- \rightarrow Co \quad (10)$$

$$CoCit^- + 2e^- \rightarrow Co + Cit^{3-} \quad (11)$$

Co-citrate complexes are only present in solutions with pH values around 5.0 and containing a large citrate concentration[24,25]. In low citrate concentration solutions, Co deposition occurs preferentially throw aquo-complexes and with a large overvoltage[24].

For Cu-Co alloys coatings, citrate concentration higher than 0.5 $mol.L^{-1}$ is needed to keep the bath stability and to produce of a Cu-Co solid solution[9]. Similar results were observed for Cu-Zn alloys coatings from citrate bath[11].

In this work, Cu-Co alloys coatings were galvanostatically electrodeposited on platinum, using a citrate-based bath as the electrolytic medium. The effects of the cathodic current density and the mechanical stirring on the current efficiency and alloy coating composition were evaluated using statistic responses. The aim of this study was to contribute to a better understanding of the Cu-Co electrodeposition process from citrate-based electrolytes in order to attain a more efficient control of the alloy coatings properties studied.

2. Experimental Procedures

2.1. Cathodic polarization curves

Cathodic polarization curves were galvanostatically obtained from baths described in Table 1, in the current density range from 0.004 to 12.48 $mA.cm^{-2}$, using a potentiostat/galvanostat system. A platinum net (Area = 5.65 cm^2) was used as the working electrode, while a platinum spiral was the counter electrode. The reference electrode was a saturated mercury (I) sulfate electrode (Hg/Hg_2SO_4), SSE. These experiments were carried out in a glass cell, at room temperature and under mechanical stirring (100 rpm). Additionally, a set of polarization curves were also produced from bath 3 (Table 1), varying the stirring speed from 0 to 400 rpm, in the same current density range and using the same system and electrodes earlier described.

2.2. Alloy electrodeposition experiments

Cu-Co alloy electrodeposition experiments were performed in solution 3 of Table 1, at room temperature and under mechanical stirring. The coatings were produced using the same system earlier described in item 2.1. The electrodeposition time was calculated using the well-known Faraday's Law[26], to produce 10 mg of Cu-Co alloy coatings, and the current efficiency was obtained from gravimetric measurements. In order to optimize the Cu-Co alloy deposition process, experimental central composite design 2^2 was employed to evaluate quantitatively the influence of the applied current density and the mechanical stirring on cathodic current efficiency and alloy composition (Table 2). Four ranges of current densities were selected to produce the Cu-Co alloys, based on the polarization curves and on the results shown earlier[27]. Table 3 shows both the codified and real entry parameters values for each range of current studied. The statistic analyses of the data were carried out with the software Statistica for Windows, release 6.0 (Statsoft).

Each alloy coating was dissolved in 20% v/v nitric acid, and analyzed by flame atomic absorption spectroscopy (FAAS) to determine the elements content.

3. Results and Discussion

3.1. Cathodic polarization curves

Figure 1 presents the cathodic polarization curves of platinum in the solutions described in Table 1, using mechanical stirring speed of 100 rpm. Although it must be pointed out that the behavior of the isolated metals in an electrodeposition process cannot be extended to their alloys[14], it can be interesting to compare the polarization responses of the two isolated metals and the alloy. It is possible to note that the alloy polarization curve lies in between the curves of the two isolated metals. Moreover, the alloy curve presents more similarity to the copper deposition, even though a small depolarization can be observed, mainly at high values of current density. The alloy curve exhibits a limit current plateau, which possibly implies that the co-deposition process is controlled by diffusion of Cu. It seems that the concentrations of both complexed and uncomplexed Cu (II) ions are extremely small at the electrode surface, while the concentrations of Co species remain close to their bulk values. El-Rehim et al.[8] and Podlaha et al.[28] reported that Cu co-deposition under limiting conditions is almost entirely due to the electroreduction of Cu (II) ions, which can indicate a smaller influence of cobalt deposition process in the alloy deposition.

A set of polarization curves of platinum were obtained from bath 3 (Table 1), using mechanical stirring speed varying from 0 to 400 rpm (Figure 2). The aims of this experiment were to select

Table 1. Chemical composition and physical-chemistry data of the electrolytes.

Bath	pH	Conductivity ($mS.cm^{-1}$)	Chemical composition ($mol.L^{-1}$)			
			$CoSO_4$	$CuSO_4$	$Na_3C_5H_6O_7$	H_3BO_3
1	6.00 ± 0.05	49.4 ± 1.3	0.24	-	0.48	0.11
2	5.01 ± 0.01	49.2 ± 0.7	-	0.16	0.48	0.11
3	4.88 ± 0.08	51.7 ± 1.4	0.24	0.16	0.48	0.11

Table 2. Central composite design 2^2 experimental matrix.

Run no.	Stirring speed	Current
1	+1	+1
2	+1	–1
3	–1	+1
4	–1	–1
5	0	0
6	0	0
7	0	0
8	$-\sqrt{2}$	0
9	$\sqrt{2}$	0
10	0	$-\sqrt{2}$
11	0	$\sqrt{2}$

Table 3. Codified and normal values of the studied parameters.

Level	Stirring speed (rpm)	Current density ($mA.cm^{-2}$)		
		Range 2	Range 3	Range 4
$-\sqrt{2}$	341	0.60	1.98	9.94
+1	300	0.53	1.77	8.84
0	200	0.35	1.24	6.19
–1	100	0.18	0.71	3.54
$\sqrt{2}$	59	0.11	0.50	2.44

the current ranges to optimize the Cu-Co alloy deposition and observe the influence of the mechanical stirring on the cathodic process. The first objective was fully attained and the selected ranges shown in Figure 2 are related to Table 3. Conversely, it was not possible to note a direct effect of the stirring speed from Figure 2, since no real tendency in the curves could be verified, mainly at current values higher than 0.18 $mA.cm^{-2}$. Therefore, this result shows the limitation of the total polarization curve technique as the unique tool to describe the cathodic process dependence on the stirring speed.

It is also interesting to note that all the polarization curves present different slopes at distinct regions, which could be associated to different deposition mechanisms[29]. At potential values higher than approximately –0.3 V_{SSE} (Region 1), a very small straight region is observed, showing that above this region the deposition process could be probably kinetic controlled. Decreasing the potential, all curves present a limit current plateau (Region 2), associated to the Cu (II) ions reduction controlled by diffusion. At potential values more negative than –0.6 V_{SSE}, a small slope (Region 3) and another limit current region (Region 4) are observed, probably related to Co (II) and/or H^+ ions reduction. Similar results have been observed earlier[8,10,19,30].

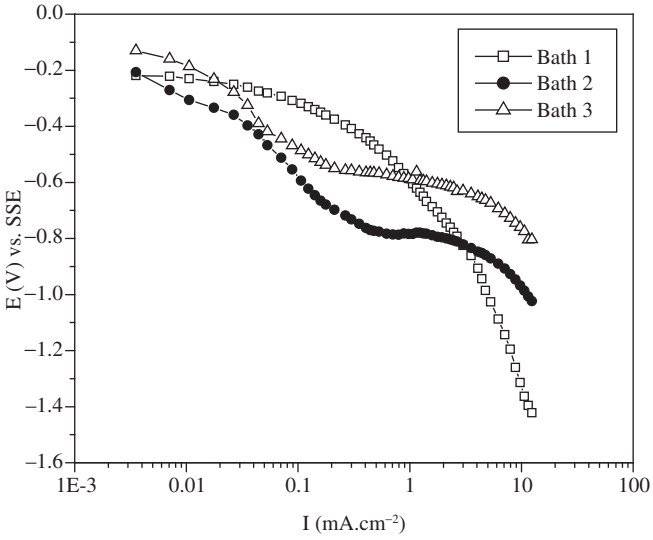

Figure 1. Cathodic polarization curves of platinum in the baths of Table 1, using mechanical stirring speed of 100 rpm.

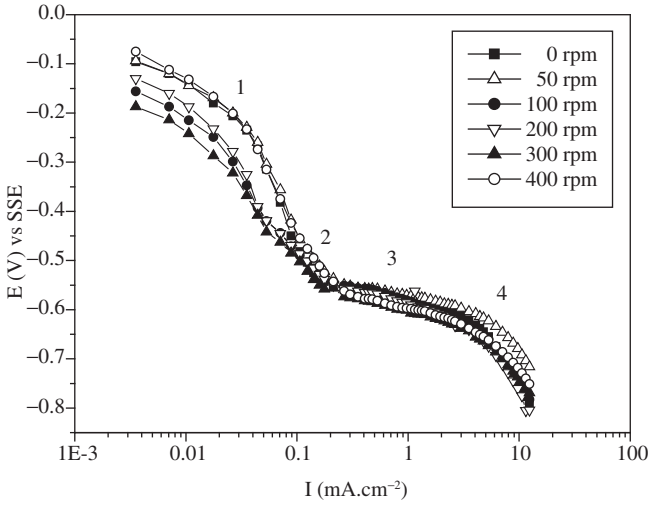

Figure 2. Cathodic polarization curves of platinum in bath 3 (Table 1).

As can be seen in Table 1, the ratio between Cu(II) and Co(II) in bath 3 is 1:1.5. This composition difference is not enough to approximate their reduction potentials and produce the alloy. In fact, the co-deposition is attained due to the complexing agent citrate ion and the different complex formation constants, K_f, for Cu(II) and Co(II) ions. Earlier reports[20-22] have showed that depending on the solution pH and on the citrate/copper ratio in the electrolyte, different copper complexes could be formed. According to the conditions showed in

Table 1 and the K_f values of all-possible copper complexes formed in bath 3, the copper hydrogenated citrate complexes (from known on represented as [Cu-CitH]), would predominate. On the other hand, a mononuclear hydrogenated cobalt citrate complex is suggested to be present at pH approximately equal to 5 and in the presence of excess of citrate[25]. Since the K_f values for citrate complexes in the pH value of solution 3 are $K_f^{Cu} = 1.62 \times 10^{14}$ and $K_f^{Co} = 6.76 \times 10^4$, respectively[31], and no large excess of citrate was added to the baths of Table 1, the cobalt deposition must probably occur from aquo-complexes [24].

3.2. Alloy electrodeposition

The effects of applied current and mechanical stirring speed could be better evaluated by applying experimental factorial procedures in the electrodeposition experiments. The main results for each current range studied, concerning the cathodic current efficiency, the contents of copper and cobalt in the coatings, and the average potential, will be shown as the effect of the parameters on these variable. Range 1 was not included since almost no alloy deposition occurred at current values below 0.07 $mA.cm^{-2}$ due to preferable hydrogen evolution on platinum cathode. After this value, the copper deposition has begun, and hydrogen overpotential increased, making it possible to produce the coating[9,16].

The complete quadratic surface model between the response and the studied factors is given by Equation 1:

$$\hat{y} = b_0 + b_1X_1 + b_2X_2 + b_{11}X_1^2 + b_{22}X_2^2 + b_{12}bX_1X_2 \quad (1)$$

where $\hat{y}$ is the estimated response, X_1 is the applied current density (I), X_2 represents the stirring speed (S), X_1X_2 is the interaction between the current density and the stirring speed (IS), and the b_i are the equation coefficients. Statistical tests ($p = 0.05$) were then used to verify if the analyzed effects present any statistical significance. Therefore, only the statistical significant effects will be represented in the final equation. It is also important to point out that even though some individuals trends could be observed on the responses (cathodic current efficiency, metal contents in the alloy, and average potential), based on the influence of the applied current density and mechanical stirring speed, the final results concerning the influence of the studied parameters were obtained by the final equation of the quadratic responses, taking into account all the significant responses observed for each effect.

The influence of the deposition parameters on cathodic efficiency for the three current ranges studied (Table 2) are shown in Table 4. It is possible to observe that this variable tends to increase with the current density range studied. It could be related to both an increasing in cobalt content with the applied current, and with the direct adsorption of copper-citrate complexes (Reactions 3 or 8), since the amount of incorporated species also increases with the applied current[20,21]. This last hypothesis seems to be corroborated by some cathodic efficiency values of 100% observed in Table 4. Figure 3 presents the fitted surface diagrams of the cathodic efficiency for the three current density ranges experienced (Table 2). Additionally, the result models obtained for the cathodic current efficiency, estimated from the experiments performed at solution 3 (Table 1) for the three studied Ranges, are represented by Equations 2, 3 and 4, respectively. It was observed, with 95% of confidence, that the main effect on the cathodic efficiency in Range 2 was the linear effect for applied current density ($p < 0.05$), and it is presented in Equation 2. Figure 3a confirms this result, since high values of current efficiency can be obtained at high current densities. Although Figure 3a also presents an apparent influence of stirring speed, this trend was not significant (ns).

$$\hat{E}f = 52 + 12\ I \quad (2)$$

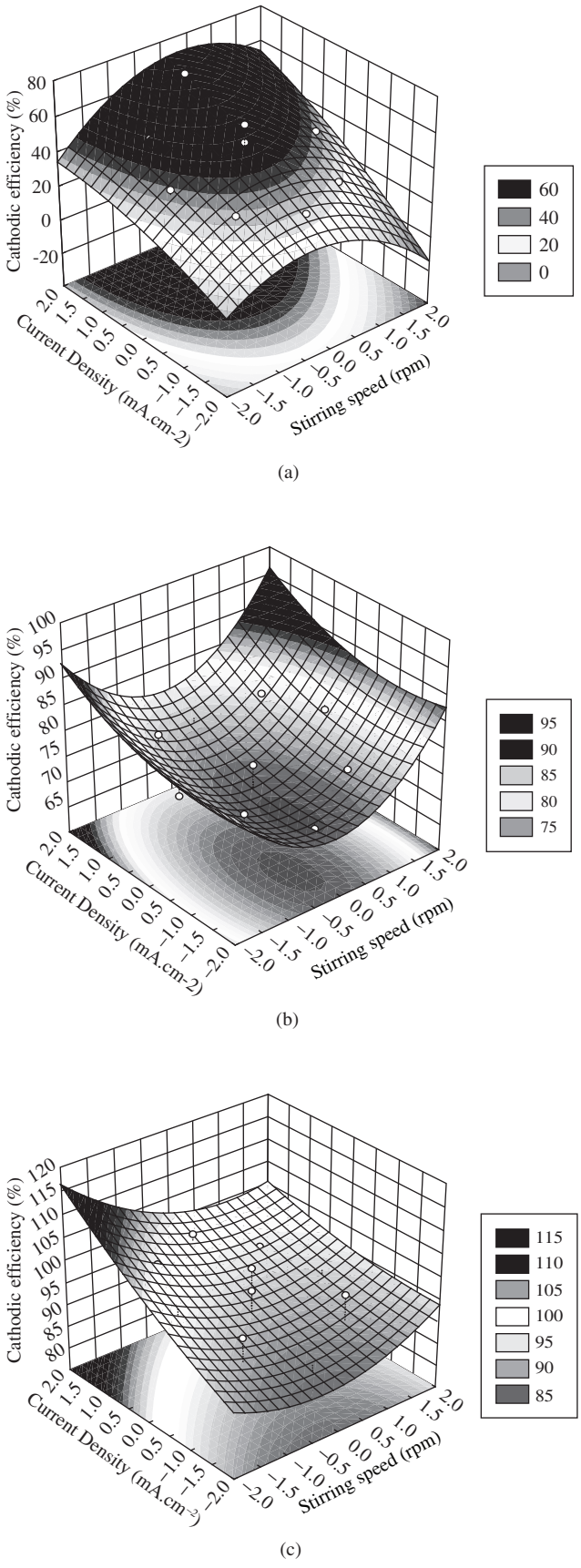

Figure 3. Fitted surfaces of standardized effects for cathodic current efficiency (Bath 3, Table 1): a) Range 2; b) Range 3; c) Range 4.

In Figures 3b and 3c, as well as the Equations 3 and 4 (Ranges 3 and 4, respectively), it is possible to see that no effect influenced significantly the cathodic efficiency (ns), except the b_0 coefficient (medium value). The fitted surface for both Ranges 3 and 4 (Figures 3b and 3c, respectively) shows only small trends of increasing the cathodic efficiency at extreme values of current density and stirring speed. Generally, the cathodic efficiency is directly related to the mass of metal in the alloy, predicted by the Faraday's Law. However, it seems that the coating formation in these two last ranges was not totally correspondent to what was expected from the Faraday's Law. The following results concerning the amount of copper and cobalt in the alloy will be correlated to these results of cathodic efficiency, in order to make this subject clearer.

$$\hat{E}f = 72 \quad (3)$$

$$\hat{E}f = 92 \quad (4)$$

Tables 5 and 6 present the responses for copper and cobalt content, respectively. Comparing the ranges, there is a tendency of increasing the amount of copper (Table 5) with the studied current density ranges (Table 2), while the cobalt content (Table 6) showed few variations. Indeed, the amount of cobalt in all experiments was always lower than 1% m/m, showing that, in the conditions in which these tests were performed, the coating must be composed almost exclusively of copper. It means that the alloy deposition in this work must be probably taking place under limiting conditions, and the influence of cobalt deposition process in the alloy is small[8,28]. Survila et al.[24] have shown that in low citrate concentration solutions, the cobalt co-deposition may occur preferentially throw aquo-complexes and at large overpotentials. Therefore, the cathodic efficiencies earlier

Table 4. Results of the variable cathodic efficiency.

Run no.	Stirring speed	Current density	Experimental condition (rpm – mA.cm^2)			Cathodic efficiency (%)		
			Range 2	Range 3	Range 4	Range 2	Range 3	Range 4
1	+1	+1	300-0.53	300-1.77	300-8.84	55	80	95
2	+1	–1	300-0.18	300-0.71	300-3.54	30	75	95
3	–1	+1	100-0.53	100-1.77	100-8.84	50	80	100
4	–1	–1	100-0.18	100-0.71	100-3.54	35	75	95
5	0	0	200-0.35	200-1.24	200-6.19	50	70	100
6	0	0	200-0.35	200-1.24	200-6.19	45	70	95
7	0	0	200-0.35	200-1.24	200-6.19	60	75	80
8	$-\sqrt{2}$	0	60-0.35	60-1.24	60-6.19	40	75	95
9	$\sqrt{2}$	0	341-0.35	341-1.24	341-6.19	40	80	90
10	0	$-\sqrt{2}$	200-0.11	200-0.50	200-2.44	30	70	80
11	0	$\sqrt{2}$	200-0.60	200-1.98	200-9.94	70	75	100

Table 5. Results of the variable copper content.

Run no.	Stirring speed	Current density	Experimental condition (rpm – mA.cm^{-2})			Copper content (% m/m)		
			Range 2	Range 3	Range 4	Range 2	Range 3	Range 4
1	+1	+1	300-0.53	300-1.77	300-8.84	27.8	37.2	4.0
2	+1	–1	300–0.18	300-0.71	300-3.54	9.0	30.5	49.2
3	–1	+1	100-0.53	100-1.77	100-8.84	27.8	53.2	57.2
4	–1	–1	100-0.18	100-0.71	100-3.54	8.0	41.2	58.5
5	0	0	200-0.35	200-1.24	200-6.19	23.8	47.8	66.5
6	0	0	200-0.35	200-1.24	200-6.19	25.0	30.0	62.5
7	0	0	200-0.35	200-1.24	200-6.19	26.5	41.2	61.2
8	$-\sqrt{2}$	0	60-0.35	60-1.24	60-6.19	39.8	67.5	89.8
9	$\sqrt{2}$	0	341-0.35	341-1.24	341-6.19	40.0	60.8	83.2
10	0	$-\sqrt{2}$	200-0.11	200-0.50	200-2.44	4.8	51.2	88.0
11	0	$\sqrt{2}$	200-0.60	200-1.98	200-9.94	60.5	70.5	89.8

Table 6. Results of the variable cobalt content.

Run no.	Stirring speed	Current density	Experimental condition (rpm – mA.cm^{-2})			Cobalt content (% m/m)		
			Range 2	Range 3	Range 4	Range 2	Range 3	Range 4
1	+1	+1	300-0.53	300-1.77	300-8.84	0.08	0.01	0.01
2	+1	–1	300-0.18	300-0.71	300-3.54	0.30	0.50	0.05
3	–1	+1	100-0.53	100-1.77	100-8.84	0.03	0.01	0.05
4	–1	–1	100-0.18	100-0.71	100-3.54	0.01	0.10	0.03
5	0	0	200-0.35	200-1.24	200-6.19	0.10	0.01	0.01
6	0	0	200-0.35	200-1.24	200-6.19	0.01	0.01	0.25
7	0	0	200-0.35	200-1.24	200-6.19	0.02	0.40	0.01
8	$-\sqrt{2}$	0	60-0.35	60-1.24	60-6.19	0.25	0.15	0.55
9	$\sqrt{2}$	0	341-0.35	341-1.24	341-6.19	0.20	0.50	0.60
10	0	$-\sqrt{2}$	200-0.11	200-0.50	200-2.44	0.20	0.15	0.28
11	0	$\sqrt{2}$	200-0.60	200-1.98	200-9.94	0.28	0.20	0.60

presented (Table 4) are mainly dependent on the copper content in the coating.

Gómez et al.[30] have shown that electrodeposition processes using complexing agents are usually useful to produce metastable Cu-Co solid solutions. In citrate baths, this can be obtained mainly with citrate solution concentration higher than 0.5 mol.L^{-1} and low polarization values[9]. Cohen-Hyams et al.[1] have shown that thin Cu-Co films presented a negligible concentration of cobalt atoms at the surface, which went through a peak concentration before gradually decreasing close to the substrate, while copper deposition followed the opposite direction. The authors suppose that copper grains are formed on the substrate and, as the deposition process progresses, the substrate changes to the Cu-Co mixture, either as a metastable solid solution and/or as nanoclusters of cobalt inside a matrix of copper. In the present work, the technique used for chemical analysis gives the total cobalt content in the alloy, and it was not able to show the cobalt distribution on the coating. Hence, new experiments are needed to reach a final conclusion about this topic.

The fitted surface diagrams (Figure 4) and the Equations 5, 6 and 7 present the results for copper content in the alloy, for the three current density ranges studied. In Range 2, both the applied current density and the stirring speed have significantly affected the copper content in the coating. The effect of the applied current density was positive and linear ($p < 0.001$), while the stirring speed showed a positive and quadratic influence on the copper content ($p < 0.04$), as shown in Equation 5. It must be pointed out that although the final response shows the quadratic influence of stirring speed for the copper content in this range, the linear effect of applied current density seems to influence predominantly the copper content in the coating, as seen in Figure 4a. It is in agreement with the p values for the estimative of the effects and their respective coefficients in Equation 5.

$$\hat{Cu\%m} / m = 25 + 15I + 3S^2 \quad (5)$$

In Range 2, the dependence of copper content on the current density can give support to Reactions 1, 6 or 7, where the direct discharge of the Cu (II) (free or complexed) on non-blocked substrate surface sites occurs. Moreover, both copper content and cathodic efficiency are linearly dependent on the applied current density, showing that, in this range, there must be a relationship between these variables. There is also a positive and quadratic influence of stirring speed on the copper content. It may imply that the Reactions above mentioned can be probably followed by the complex dissociation and the consequent removing of blocking species such as Cit^{3-} from the electrode surface (Reactions 2, 4 or 7)[20,21]. Chaissang et al.[20] have shown that the direct incorporation of the $[CuCitH]^{2-}$ complexes increased with the applied current density. As Range 2 comprises from 0.11 to 0.60 mA/cm^2, and the copper content in this Range is positively affected by mechanical stirring, it is possible to suppose that the dissociation of copper-citrate complexes (Reaction 2) may follow the charge transfer process (Reactions 1, 6 or 7) predominantly in this range. Then, when the stirring speed increases, the $[Cit^{3-}]$ species can probably be carried to the bulk and complex other metallic ions (Reaction 4).

Table 5 shows that copper content increases from Range 2 to Range 3. However, there was no significant influence (ns) of both the applied current density and stirring speed on the copper content in the coating, except the b_0 coefficient (Figure 4b and Equation 6) for Range 3. Reminding Table 4 and Equation 3, a similar result was observed for cathodic efficiency in this Range. Since the current density varies from 0.50 to 1.98 mA.cm^{-2}, the [Cu-CitH] complexes adsorption process (Reactions 3 and 8) must possibly occur without being limited by the charge transfer Reactions, and copper can be present on the substrate in the metallic form or as an incorporated

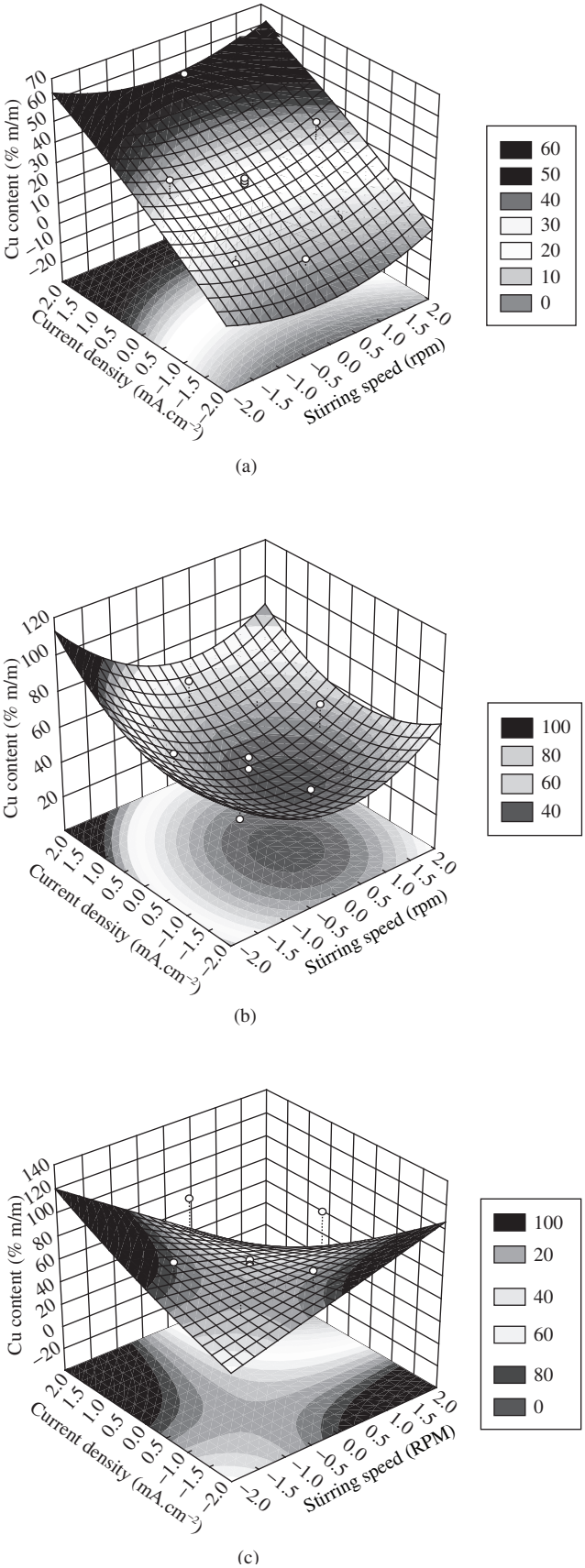

Figure 4. Fitted surfaces of standardized effects for copper content (Bath 3, Table 1): a) Range 2; b) Range 3; c) Range 4.

complex. This tends to occur mainly at low stirring speeds, where the adsorbed species may not be removed from the electrode surface, and at high current density values, where the direct adsorption of the complex is enhanced. In Range 3, Reactions 3 or/and 8 must, probably, be favored by the applied current density range, as proposed by both Chaissang et al.[20] and Rode et al.[21].

$$\hat{Cu\%m} / m = 40 \quad (6)$$

Concerning Range 4, there is a linear, significant, and negative influence of both current density ($p < 0.03$) and stirring speed ($p < 0.01$) on the copper content in the coating. Moreover, there is a joint and negative effect of both deposition parameters ($p < 0.02$) on this variable (Figure 4c, and Equation 7). Figure 5 shows the surface response for this model and it indicates that, in this range, copper deposition was disfavored only by a simultaneous increase or simultaneous decrease of both current density and stirring speed. It can also be observed in Equation 7. An alternate increase of them (that is, in conditions where small current densities and high stirring speeds, or high current density values and low stirring speeds are applied), the amount of copper tends to increase. Both Chaissang et al.[20] and Rode et al.[21] have shown that the increase in current density values favors the direct incorporation of Cu-Citrate complexes, while the blocking species are removed by increasing the stirring speed. Therefore, the combination of low stirring speeds and high current densities may probably enhance the direct incorporation of copper as Cu-citrate complexes on the electrode surface, while the joint effect of low current density and high stirring speed may stimulate the direct reduction of Cu (II) species, since any blocking species as $Cit^{3-}_{(ads)}$ can be removed from the electrode surface (Reaction 4).

$$\hat{Cu\%m} / m = 64 - 5.5I - 9.0S - 11IS \quad (7)$$

Table 7 shows the variation of the average potential attained at each different condition applied to the electrodeposition process. It can be noted that the potential becomes more negative as the current density increases from Range 2 to Range 4, as it was expected. Moreover, the results seem to be more dependent on the current density than on the stirring speed, which can be confirmed by the statistical analysis. The fitted surfaces for Ranges 2 and 3 are presented in Figures 5a and 5b, respectively. It is clear that, in both cases, more negative potentials were obtained increasing the current density values, no matter the stirring speed used. These results are also shown in Equations 8 and 9.

$$\hat{E}_{SSE} = -0.577 - 0.022I + 0.015I^2 \quad (8)$$

$$\hat{E}_{SSE} = -0.617 - 0.017I + 0.007I^2 \quad (9)$$

Both Equations show that this influence of current density is negative and linear ($p < 0.003$ for both ranges), as well as positive and quadratic ($p < 0.01$ and $p < 0.02$, for Ranges 2 and 3, respectively). The p values confirm that the quadratic effect is smaller that the linear one, which agrees with Figures 5a and 5b. However, Equations 8 and 9 suggest that at extremely high values of current density (out of the studied ranges), a depolarization might be observed in both cases. Both copper content and cathodic efficiency increase with the current density in Range 2, while the potential becomes more negative. The significant decrease of potential with the increase of current density in this range can be associated to the Cu (II) ions reduction controlled by diffusion, as seen in the polarization curves (Figure 2), and may be probably related to Reactions 1, 2, 6 or 7.

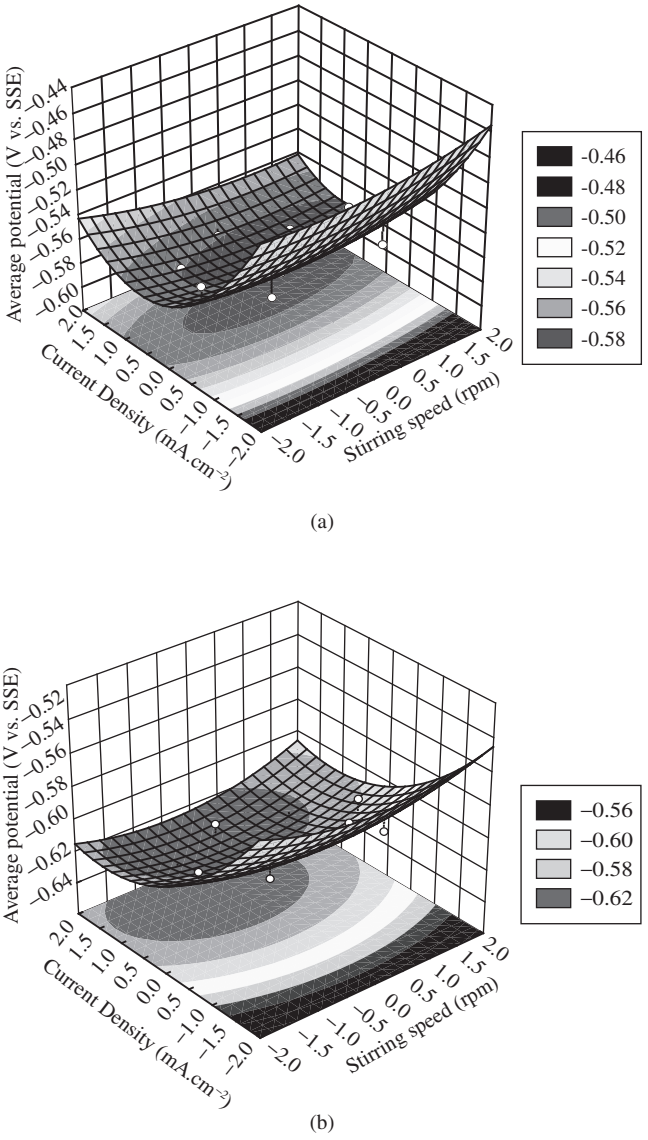

Figure 5. Fitted surfaces of standardized effects for average potential (Bath 3, Table 1) a) Range 2; and b) Range 3.

At Region 3, the polarization curves (Figure 2) show a very small slope, and the influence of current density on potential was significant, even though there was no influence of this parameter on cathodic efficiency, copper content, or even cobalt content. There was a tendency on increasing copper content at high current densities and low stirring speed, which has been related to a probable incorporation of Cu-Citrate complex. Apparently, this potential variation may not be related to metal deposition. It could probably be connected to a parallel reaction, like hydrogen reduction, or to an overpotential due to the presence of an adsorbed blocking species on the surface. However, more experiments are needed to reach a final conclusion about this topic.

On the other hand, there was no significant effect (ns) of both deposition parameters on potential for Range 4 (not shown). In this range, there was a significant influence of the studied deposition parameters on copper content in the alloy, enhancing the direct incorporation of Cu-Citrate complexes on the electrode surface. This phenomenon seems to present no relationship to the average deposition potential and needs to be studied more carefully.

Table 7. Results of the variable Average Potential.

Run no.	Stirring speed	Current density	Experimental condition (rpm – mA.cm^{-2})			Average potential (V vs. SSE)		
			Range 2	Range 3	Range 4	Range 2	Range 3	Range 4
1	+1	+1	300-0.53	300-1.77	300-8.84	–0.585	–0.629	–0.782
2	+1	–1	300-0.18	300-0.71	300-3.54	–0.553	–0.559	–0.669
3	–1	+1	100-0.53	100-1.77	100-8.84	–0.580	–0.631	–0.768
4	–1	–1	100-0.18	100-0.71	100-3.54	–0.557	–0.598	–0.670
5	0	0	200-0.35	200-1.24	200-6.19	–0.573	–0.620	–0.719
6	0	0	200-0.35	200-1.24	200-6.19	–0.578	–0.615	–0.669
7	0	0	200-0.35	200-1.24	200-6.19	–0.580	–0.617	–0.722
8	$-\sqrt{2}$	0	60-0.35	60-1.24	60-6.19	–0.564	–0.606	–0.704
9	$\sqrt{2}$	0	341-0.35	341-1.24	341-6.19	–0.564	–0.602	–0.695
10	0	$-\sqrt{2}$	200-0.11	200-0.50	200-2.44	–0.495	–0.572	–0.612
11	0	$\sqrt{2}$	200-0.60	200-1.98	200-9.94	–0.581	–0.622	–0.754

4. Conclusions

The results of polarization curves showed the limitation of this technique as the unique tool to evaluate the effects of the deposition parameters studied (applied current density and mechanical stirring speed) on the cathodic efficiency, metal contents in the alloy coatings, and average deposition potential. The use of a statistical approach allowed a better understanding of the effect of these parameters on the studied variables, making it possible to corroborate the results with the mechanisms proposed, mainly by Chaissang et al.[20] and Rode et al.[21].

The variance analysis (ANOVA) for the cathodic efficiency indicated that 79.47% of the results obtained for Range 2 can be explained for the model, while values of 51.36 e 34.78% were found for Ranges 3 and 4, respectively. For copper and cobalt contents in the alloy, and for the average potential, the amount of results explained by the model were much slower than those found for cathodic efficiency. It means that applied quadratic model needs to be better adjusted to represent correctly the experimental data.

Acknowledgments

The authors would like to thank UERJ, FAPERJ, and Prociência Program for the financial support.

References

1. Cohen-Hyams T, Kaplan WD, Aurbach D, Cohen YS, Yahalom J. Electrodeposition of granular Cu-Co alloys. *Journal of the Electrochemical Society.* 2003; 150 (1): C28-C35.
2. Jyoko Y, Kashiwabara S, Hayashi Y. Preparation of giant magnetoresistance Co–Cu heterogeneous alloys by electrodeposition. *Journal of the Electrochemical Society*. 1997; 144(7): L193-L195.
3. Jyoko Y, Kashiwabara S, Hayashi Y. Preparation of giant magnetoresistance Co/Cu multilayers by electrodeposition. *Journal of the Electrochemical Society.* 1997; 144(1): L5-L8.
4. Mohamed AE, Rashwan SM, Abdel-Wahaab SM, Kamel, MM. Electrodeposition of Co-Cu alloy coatings from glycinate baths. *Journal of Applied Electrochemistry*. 2003; 33(11): 1085-1092.
5. Endoh E, Otouma T, Morimoto T, Oda Y. New Raney nickel composite-coated electrode for hydrogen evolution. *International Journal of Hydrogen Energy.* 1987; 12(7): 473-479.
6. Vermeiren P, Leysen R, Vandenborre H. Study of hydrogen evolving reaction in alkaline medium at nickel and cobalt based electrocatalysts. *Electrochimica Acta.* 1985; 30 (9): 1253-1255.
7. Crousier J, Bimaghra I. Effect of nickel on the electrodeposition of copper. *Journal of Applied Electrochemistry.* 1993; 23(8): 775-780.
8. Abid El-Rehim S S, Abd El-Wahab SM, Rashwan, SM, Anwar ZM. Electroplating of a Cu-Co alloy from a citrate bath containing boric acid. *Journal of Chemical Technology and Biotechnology*. 2000; 75(3): 237-244.
9. Antón RL, Fdez-Gubieda ML, García-Arribas A, Herreros J, Insausti M. Preparation and caracterisation of Cu–Co heterogeneous alloys by potenciostatic electrodeposition. Materials Science and Engineering A. 2002; 335(1-2): 94-100.
10. de Farias LT, Luna AS, Senna LF, do Lago DCB. In: Luz Jr, LFL. editor. Eletrodeposição de ligas cobre-cobalto. Proceedings of 15th Brazilian Congress of Chemical Engineering; 2004 Sep. 26 - 29. Curitiba, Brazil. 2004. CD-ROM.
11. Ferreira FBA, Silva FLG, Luna AS, Lago DCB, Senna LF. Response surface modeling and optimization to study the influence of the deposition parameters on the electrodeposition of Cu-Zn alloys in citrate medium. Journal of Applied Electrochemistry. 2007; 37(4): 473-471.
12. Santana RAC, Prasad S, Campos ARN, Araújo FO, da Silva GP, de Lima-Neto P. Electrodeposition and corrosion behaviour of a Ni-W-B amorphous alloy. *Journal of Applied Eletrochemistry.* 2006; 36(1): 105-113.
13. San Martín V, Sanllorente S, Palmero S. Optimization of influent factors on nucleation process of copper in solutions containing thiurea using an experimental design. *Electrochimica Acta*. 1998; 44(4): 579-585.
14. Vagramyan TA. In: Kruglikov SS, editor. *Electrochemistry*. Jerusalem: Israel Program of Scientific Translation Ltd.; 1970.
15. Senna LF, Díaz SL, Sathler L. Electrodeposition of copper-zinc alloys in pyrophosphate-based electrolytes. *Journal of Applied Electrochemistry*. 2003; 33(12): 1155-1161.
16. Lainer VI. *Modern electroplating*. Jerusalem: Israel Program of Scientific Translation Ltd; 1970.
17. Fujiwara Y, Enomoto H, Electrodeposition of β'-brass from cyanide baths with accumulative underpotential deposition of Zn. *Journal of the Electrochemical Society*. 2000; 147(5): 1840-1846.
18. Fujiwara Y, Enomoto H. Electrodeposition of Cu/Zn alloys from glucoheptanate baths. *Surface Coating and Technology.* 1988; 35(1-2): 101-11.
19. Gómez E, Llorente A, Alcobe X, Vallés E. Electrodeposition for obtaining homogeneous or heterogeneous cobalt-copper films. *Journal of Solid State Electrochemistry*. 2004; 8(2): 82-88.

20. Chassaing E, Quang KV, Wiart R. Kinetics of copper electrodeposition in citrate electrolytes. *Journal of Applied Electrochemistry*. 1986; 16(4): 591-604.

21. Rode S, Henninot C, Vallières C, Matlosz M. Complexation chemistry in copper plating from citrate baths. *Journal of the Electrochemical Society*. 2004; 151(6): C405-C411.

22. Uksene V, Survila A, Zukauskaitè A. The electroreduction mechanism of copper (II) citrate complexes. *Russian Journal of Electrochemistry*. 1996; 32(8): 950-965.

23. Gómez E, Ramirez J, Vallés E. Electrodeposition of Co-Ni alloys. *Journal of Applied Electrochemistry*. 1988; 28(6): 71-79.

24. Survila A, Mockus Z, Kanapeckaité S. Kinetics of Sn and Co codeposition in citrate solutions. *Electrochimica Acta*. 2000; 46(4): 571-577.

25. Kotsakis N, Raptopoulou CP, Tangoulis V, Terzis A, Giapintzakis J, Jakusch T, Kiss T, Salifoglou A. Correlations of synthetic, spectroscopic, structural, and speciation studies in the biologically relevant cobalt(II)-citrate system: the tale of the first aqueous dinuclear cobalt (II)-citrate complex. *Inorganic Chemistry*. 2003; 42(1): 22-31.

26. Christian GD, O'Reilly EJ. *Instrumental Analysis*. Boston: Allyn & Bacon, Inc; 1986.

27. Lago DCB, Senna LF, Afonso PKC, de Farias LT. *Estudos preliminares do processo de eletrodeposição de ligas Cu–Co. Proceedings of the 7th Conference of Equipments Technology;* 2003 Dec. 9-12. Florianópolis, Brazil. 2003. CD-ROM.

28. Podlaha ELJ, Bonhote CH, Landolt DA. Mathematical model and experimental study of the electrodeposition of Ni-Cu alloys from complexing electrolytes. *Electrochimica Acta*. 1994; 39 (18): 2649-2657.

29. Greef R, Peat R, Peter LM, Pletcher D, Robinson J. *Instrumental Methods in Electrochemistry*. London: Ellis Horwood Limited; 1985.

30. Gómez E, Llorente A, Vallés E. Obtention and characterisation of cobalt + copper electrodeposits from a citrate bath. *Journal of Electroanalytical Chemistry*. 2000; 495(1): 19-26.

31. Lurie Ju, *Handbook of analytical chemistry*. Moscow: Mir Publishers; 1978.